Available online www.worldscientificnews.com

World Scientific News

An International Scientific Journal

WSN 218 (2026) 159-175 EISSN 2392-2192

Synthesis and Mesomorphic Behavior of Azo-Cinnamate Containing Highly Polar Pyridine Derivatives

P. R. Hadiya *[a], U. C. Bhoya[a]

[a]Department of Chemistry, Saurashtra University, Rajkot, India – 360005

Email*: poonamhadiya1511@gmail.com

https://doi.org/10.65770/VNFC9007

ABSTRACT

A new azo-based liquid crystalline compound, 4-(4'-n-alkoxy-3'-methoxy cinnamyloxy) phenyl azo-5''-(2''-cyano-3''-trifluoromethyl) pyridine, was synthesized and characterized. The structure was confirmed by elemental analysis, FT-IR, and NMR spectroscopy. The molecular design, incorporating azo and ester linkages along with polar –CN and $–CF_3$ substituents on the pyridine ring, enhances molecular anisotropy and intermolecular interactions. Mesomorphic properties studied by polarizing optical microscopy (POM) and differential scanning calorimetry (DSC) revealed the presence of stable nematic and smectic phases. The results indicate that these compounds exhibit good thermal stability and are promising for applications in liquid crystal and photonic devices.

Keywords: Pyridine, Mesomorphism, Smectic, Nematic, Liquid Crystal, Azo-cinnamate, Pyridine Derivatives.

(Received 8 June 2026; Accepted 20 July 2026; Date of Publication 31 August 2026)

1. INTRODUCTION

Liquid crystals (LCs) represent a unique class of materials that exhibit properties intermediate between those of crystalline solids and ordinary isotropic liquids.[1] In such systems, the molecules maintain a certain degree of orientational order similar to that found in crystalline structures, while still retaining the ability to flow like a conventional liquid.[2] This partially ordered state arises mainly from the anisotropic nature of the molecules, which encourages alignment in a preferred direction without enforcing complete positional order.[3] Owing to this combination of structural organization and fluidity, liquid crystalline materials have become an important subject of scientific investigation.[4]

Liquid crystalline systems are commonly divided into two principal categories: thermotropic and lyotropic liquid crystals.[5] Thermotropic liquid crystals exhibit mesomorphic phases as a result of temperature variation, whereas lyotropic liquid crystals develop ordered structures through the interaction of amphiphilic molecules with a suitable solvent.[6]Among these types, thermotropic liquid crystals have been studied more extensively because of their structural versatility and their significant role in various electro-optical applications.[7]

The intermediate phase that occurs between the crystalline solid and the isotropic liquid is known as the mesophase, and substances capable of forming such phases are referred to as mesogenic compounds.[8] Several types of mesophases may be observed depending on the extent and nature of molecular arrangement, including nematic, smectic, and cholesteric phases.[9] The occurrence and stability of these mesophases largely depend on molecular design, particularly the presence of rigid aromatic cores, flexible alkyl chains, and linking groups such as ester, azo, or imine functionalities.[10]

Liquid crystalline materials have attracted considerable attention due to their distinctive optical and electrical properties.[11] These materials play a significant role in modern technologies and are widely utilized in liquid crystal display devices, optical switching systems, sensors, and other advanced photonic applications.[12] As a result, the synthesis and detailed study of new mesogenic compounds have become an active and important field of research in materials science.[13]

Phenyl derivatives containing heterocyclic units have also been synthesized, and they have attracted increasing research interest in recent years.[14] This is mainly because heteroatoms play a key role in enhancing the formation and stability of mesophases, and heterocyclic structures allow the development of a wide variety of mesogenic materials [15]. The incorporation of heteroatoms such as sulfur (S), oxygen (O), and nitrogen (N) can strongly influence mesogenic properties, including the nature of the mesophase, transition temperatures, and dielectric behaviour [16]. Moreover, these heteroatoms can affect molecular polarity, polarizability, and sometimes even the molecular shape [17]. Common heterocyclic rings used as central cores in liquid crystal systems include pyridine [18], 1,3,4-thiadiazole [19], thiophene [20], and benzothiazole [21].

In response to the increasing research interest in heterocyclic liquid crystalline materials, a series of pyridine-based azoester liquid crystals was synthesized. [22] Pyridine is structurally related to benzene, as one of the –CH groups in the benzene ring is replaced by a nitrogen heteroatom. [23] However, pyridine possesses slightly lower resonance stabilization compared with benzene. The present study focuses on the synthesis of a homologous series in order to investigate the influence of molecular structure on the liquid crystalline properties of pyridine-containing azo ester derivatives. [24]

The designed molecular framework consists of an alkoxy terminal chain, ester and azo linking groups, along with a para-substituted –CN lateral group on the pyridine ring and a meta-substituted –CF_3 group . The obtained thermometric data are analyzed to understand how molecular rigidity and flexibility influence the mesomorphic behaviour of the synthesized compounds.[25]

2. EXPERIMENTAL

Synthesis

Synthesis of 4-n- alkoxy 3 -methoxy cinnamic acid (Int-1)

4-*n*-Alkoxy3-methoxybenzaldehydes were synthesized by refluxing 4-hydroxy 3-methoxy benzaldehyde (1 equiv.) with corresponding n-alkyl bromides (1 equiv.) in the presence of potassium carbonate (1 equiv.) and DMF as a solvent . The resulting 4-n-alkoxy 3-methoxy benzaldehydes were reacted with malonic acid (1.2 equiv.) in the presence of 1-2 drops piperi dine as catalyst and pyridine as solvent to yield corresponding trans-4-n-alkoxy 3-methoxy cinnamic acids [A].[26]

Synthesis of 4-hydroxy phenyl azo-5'(2'-cyano-3'-trifluoro methyl) pyridine (Int-2)

The synthesis of the azo dye intermediate, 4 hydroxy phenyl azo5'(2'- cyano 3'- trifluro methyl pyridine (mp 125^{o}C yield 75%), was synthesized via conventional diazotization of 5 amino -3-trifluoro methyl picolinonitryl using sodium nitrite in acidic medium, followed by coupling with phenol.[27]

Synthesis of 4-(4'-n-alkoxy-3'-methoxy cinnamyloxy) phenyl azo-5''-(2''-cyano-3''-trifluoromethyl) pyridine

The final azoester derivatives were prepared by Steglich esterification of the alkoxy acids with the azo dye using dicyclohexylcarbodiimide (DCC) and 4-dimethylaminopyridine (DMAP) as coupling agents. The crude products were recrystallized and purified repeatedly until constant and sharp phase transition temperatures were observed, which were confirmed using a polarizing optical microscope equipped with a temperature-controlled heating stage. All starting materials, including 4-hydroxy 3-methoxy benzaldehyde, alkyl halides, malonic acid, 5- amino 3-trifluoromethyl picolinonitryl, phenol, NaOH, KOH, $NaNO_2$, and esterification reagents, were used as received without further purification, whereas solvents such as methanol and dichloromethane (DCM) were dried and distilled prior to use to maintain anhydrous conditions.[28] The overall synthetic route is depicted in Scheme 1.

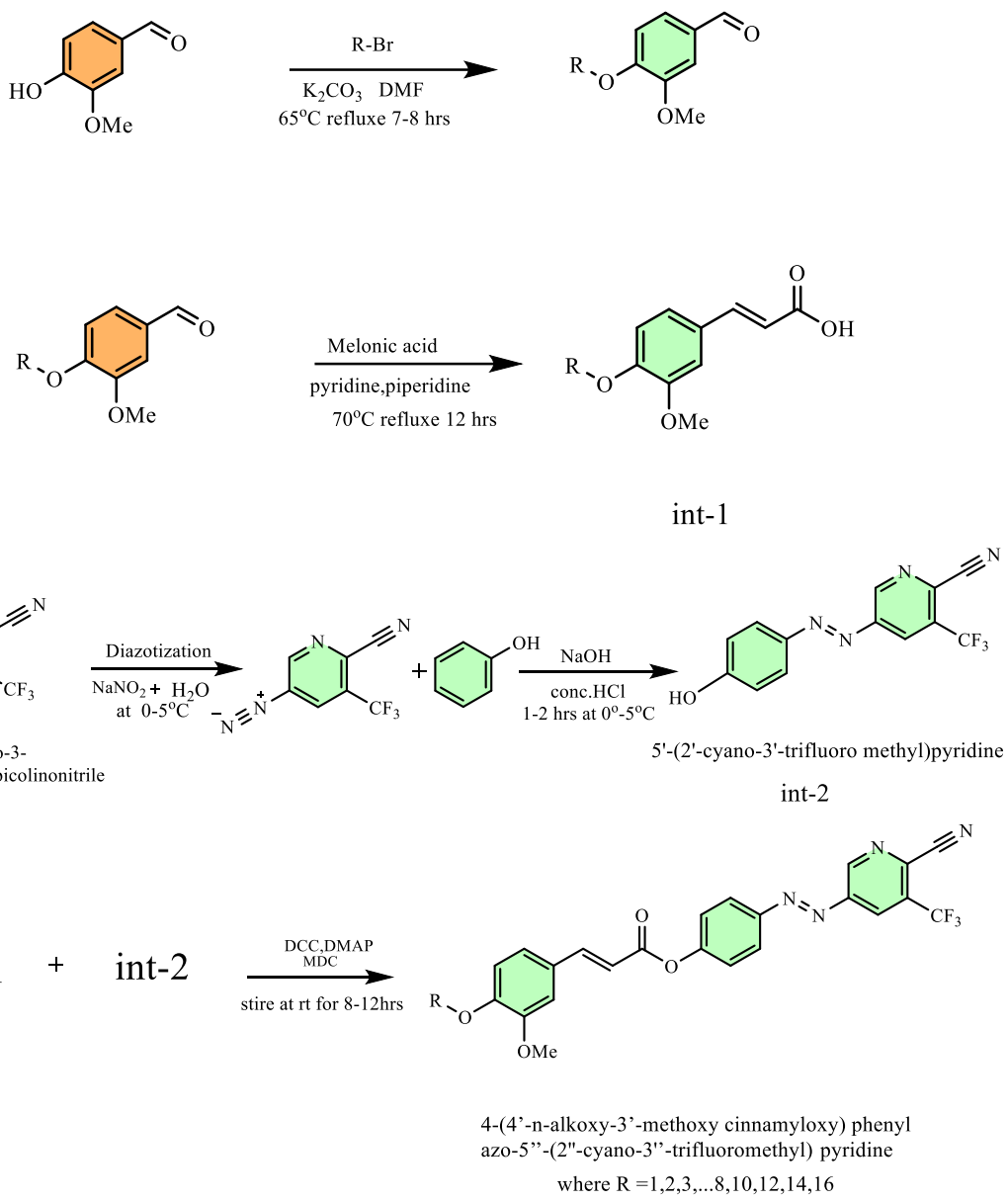

Charectarization

Selected members of the series were characterized using elemental analysis on a EuroEA Elemental Analyzer (Table 1). FT-IR spectra were recorded using a Shimadzu FTIR-8400 spectrometer in the range of 4000-400 CM^{-1}, while ^1H NMR spectra were obtained on a Bruker Avance Neo 600 MHz NMR spectrometer with $CDCl_3$ as the solvent. Mass spectra were recorded using a Shimadzu GC-MS ultra (Model: QP-2010). The thermal behavior of the compounds was analyzed using a Differential Scanning Calorimeter (Shimadzu DSC-60, Singapore, version 10.8). Additionally, mesomorphic properties were examined using polarized optical microscopy (POM) on a Nikon Eclipse 400/TU Plan ELWD 20X/0.40 microscope. In such series, the molecular core structure remains constant, with variation only in the terminal alkyl chain length. Therefore, structural confirmation of a few representative members is considered sufficient to validate the entire series. This is a widely accepted approach in the characterization of liquid crystalline homologues.

3. ANALYTICAL DATA

IR in cm^{-1} for pentytyloxy derivative (D_5)

3244.71 (aromatic C–H stretching), 2979.64 (aliphatic C–H stretching of alkoxy chain), 2215.71 (C≡N stretching of cyano group), 1607.47 (C=O stretching of ester –COO– group), and 1559.07 (aromatic C=C stretching), 1414.40 (–N=N– azo stretching), 1350.09 and 1313.51 (aromatic C–C vibrations), 1274.40 (C–O stretching of ester linkage), 1214.36, 1151.48, and 1117.45 (C–F stretching of $–CF_3$ group), 1072.68 (C–O stretching), 872.28 and 823.24 (para-disubstituted benzene ring vibration), 791.45, 721.15, and 691.56 (aromatic C–H out-of-plane bending), 597.86, and 518.68 (fingerprint region vibrations). The IR data are consistent with the molecular structure. IR in cm^{-1} for pentyloxy derivative.

IR in cm^{-1} for octyloxy derivative (D_8)

2980.39 (C–H stretching of alkyl/alkoxy chain), 2210.40 (C≡N stretching of cyano group), 1610.98 and 1559.65 (aromatic C=C stretching), 1507.72 and 1415.98 (–N=N– azo linkage vibration), 1349.41 and 1314.94 (aromatic skeletal vibration), 1273.07 (C–O stretching of ester –COO– group), 1076.40 and 1007.88 (C–O stretching), 872.07 and 822.99 (para-disubstituted benzene ring), 793.63 and 715.58 (aromatic C–H out-of-plane bending), 669.69 and 599.19 cm^{-1} (fingerprint region vibrations).

^{1}H NMR in ppm of ethoxy derivative (D_2)

^{1}H NMR (400 MHz, $CDCl_3$) δ 9.43 (d, *J* = 2.1 Hz, 1H pyridine ring near -CF_3), 8.53 (d, *J* = 2.1 Hz, 1H near pyridine ring), 8.11 (d, *J* = 8.6 Hz, 2H second phenyl ring near -N=N-), 7.88 (d, *J* = 15.8 Hz, 1H near third phenyl ring -CH=CH-), 7.44 (d, *J* = 8.5 Hz, 2H second phenyl ring), 7.20 (dd, *J* = 8.2, 2.0 Hz, 1H third phenyl ring near -OCH_3), 7.15 (s, 1H third phenyl), 6.93 (d, *J* = 8.3 Hz, 1H third phenyl ring 6.53 (d, *J* = 15.8 Hz, 1H -CH=CH- near -COO-), 4.19 (q, *J* = 6.9 Hz, 2H of -OCH_2), 3.97 (s, 3H of -OCH_3), 1.53 (t, *J* = 7.0 Hz, 3H of -OC_2H_5).

^{1}H NMR in ppm of decyloxy derivative (D_{10})

^{1}H NMR (400 MHz, $CDCl_3$) δ 9.43 (d, *J* = 2.1 Hz, 1H pyridine ring near -CF_3), 8.53 (d, *J* = 2.2 Hz, 1H near pyridine ring), 8.11 (d, *J* = 8.8 Hz, 2H second phenyl ring near -N=N-), 7.89 (d, *J* = 15.9 Hz, 1H near third phenyl ring -CH=CH-), 7.58 (d, *J* = 8.7 Hz, 2H second phenyl ring), 7.45 (dd, *J* = 8.7, 4.1 Hz, 1H third ring near-OCH_3), 7.18 (s, 1H third phenyl ring), 6.63 (d, *J* = 15.3 Hz, 1H third phenyl ring), 6.53 (d, *J* = 15.9 Hz, 1H -CH=CH- near -COO-), 4.18 – 3.96 (m, 4H), 3.77 (d, *J* = 10.0 Hz, 1H), 2.01 (tt, *J* = 11.4, 7.3 Hz, 4H), 1.91 – 1.69 (m, 6H), 1.55 – 1.33 (m, 10H), 1.31 (s, 16H), 1.32 – 1.15 (m, 8H), 1.13 (s, 1H), 0.91 (td, *J* = 6.8, 2.4 Hz, 5H).

Mass spectra of propyloxy derivative(D_3)

m/z (rel.int%):511.2(M^+)

Mass spectra of hexyloxy derivative(D_6)

m/z (rel.int%):550.2(M)

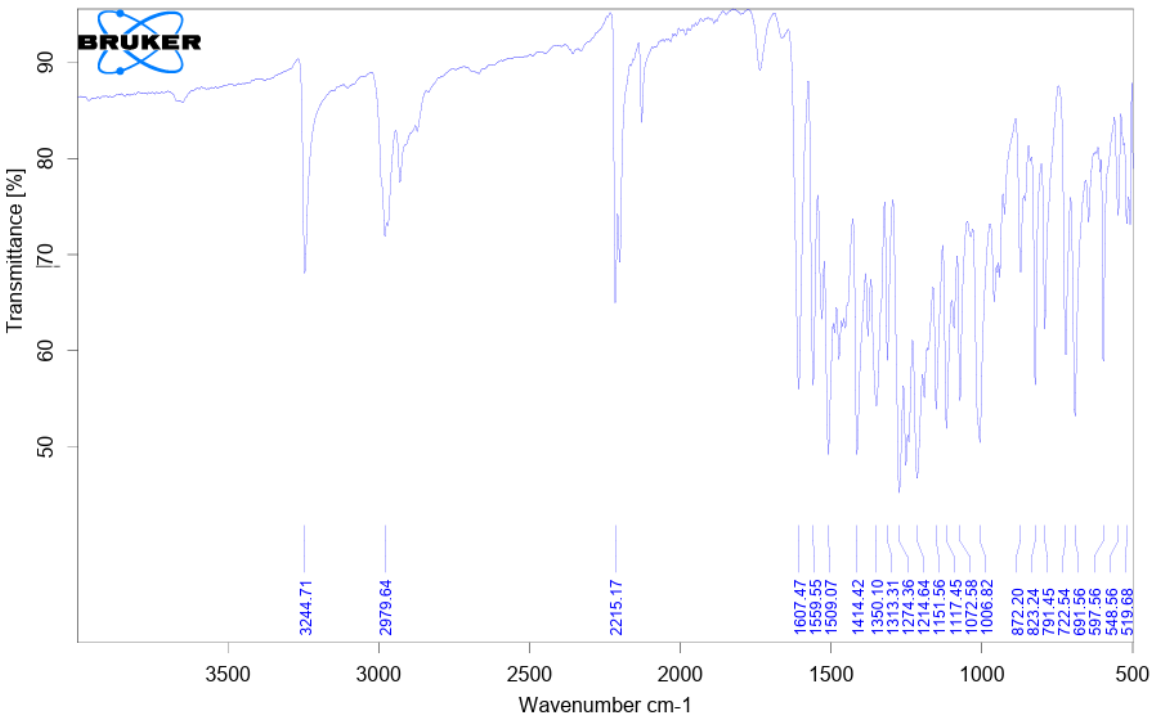

IR in cm^{-1} for pentytyloxy derivative (D$_5$)

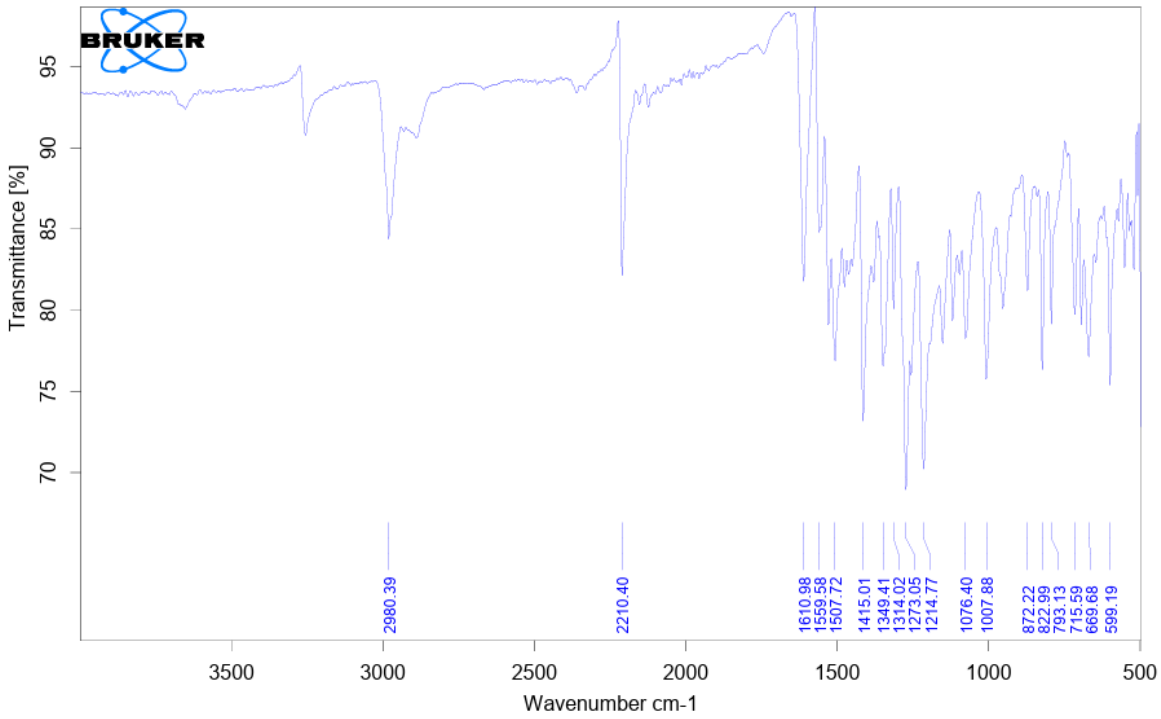

IR in cm^{-1} for octyloxy derivative (D$_8$)

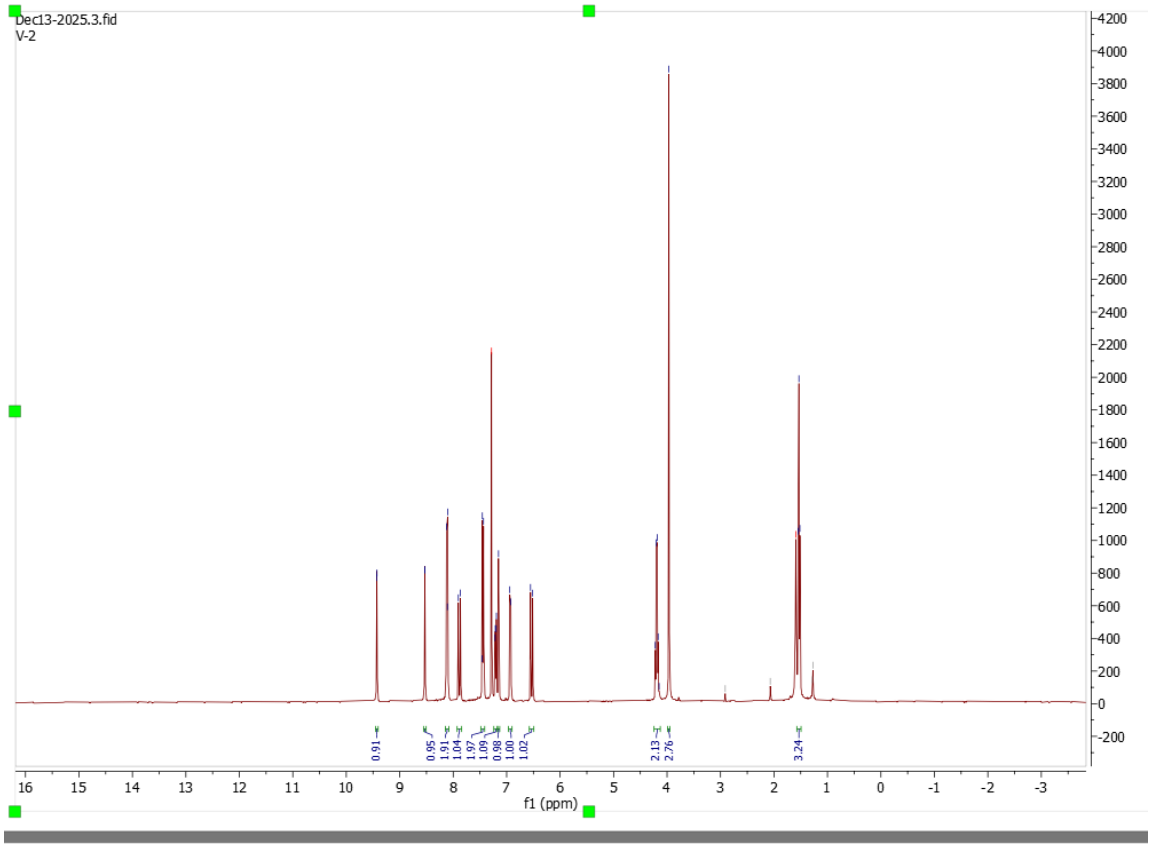

^{1}H NMR in ppm of ethoxy derivative (D_2)

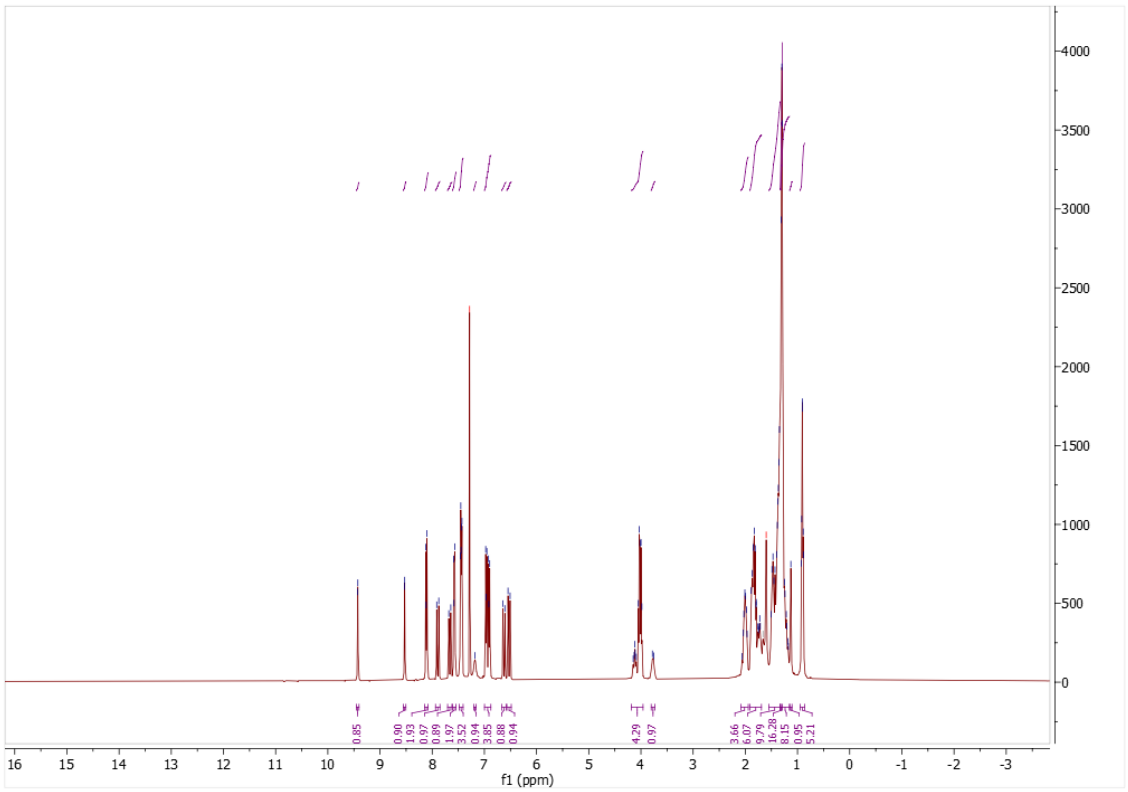

^{1}H NMR in ppm of decyloxy derivative (D_{10})

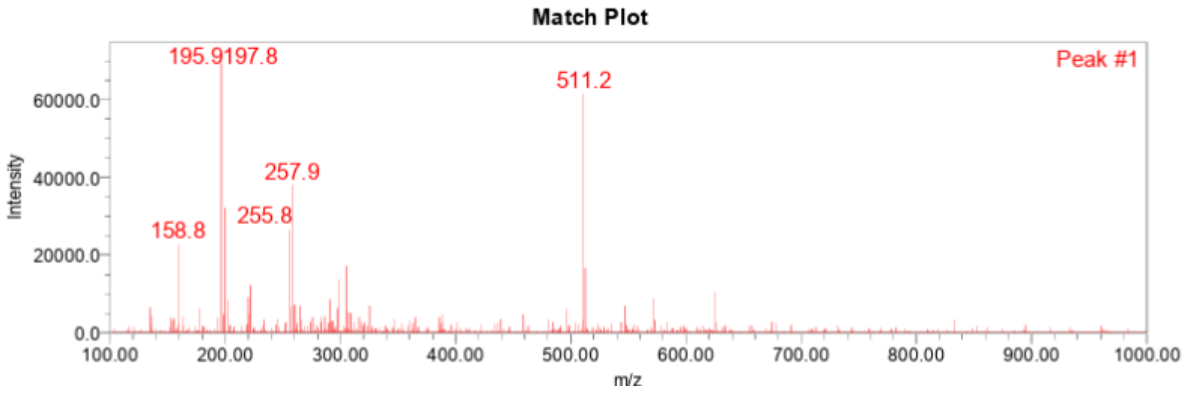

Mass spectra of propyloxy derivative(D_3)

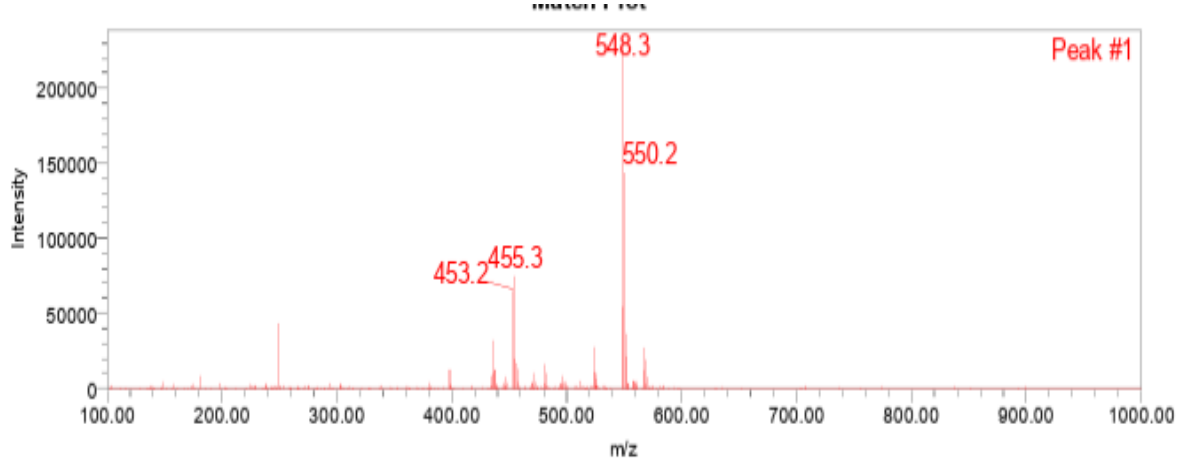

Mass spectra of hexyloxy derivative(D_6)

Table 1. Elemental Analysis.

Sr no.	Molecular formula	Elements% calculated					Elements% found				
		C	H	O	N	F	C	H	O	N	F
1	$C_{24}H_{17}F_3N_4O_4$	59.75	3.55	13.27	11.61	11.81	59.45	3.33	12.26	11.33	11.37
2	$C_{25}H_{19}F_3N_4O_4$	60.48	3.86	12.89	11.29	11.48	60	3.43	11.9	11.72	11.44
3	$C_{26}H_{21}F_3N_4O_4$	61.18	4.15	12.54	10.98	11.17	60.79	3.77	11.56	10.33	11.13

4. RESULT AND DISCUSSION

A homologous series of new azo cinnamoyl esters, synthesized from trans 4-n-alkoxy-3-methoxy cinnamic acid and 4-hydroxy phenyl azo 5'(2'-cyano 3'-trifluoro methyl) pyridine as shown in Scheme 1, exhibits thermotropic liquid crystalline behavior. This series comprises 12 members, C_1 to C_{16}. C_1 to C_5 are non mesomorphic, while C_6 to C_{16} homologues show enantiotropic smectic and nematic phases. Transition temperatures determined via polarizing optical microscopy in heating cycle (Table 2) were plotted against the number of carbon atoms in the n-alkyl chain of the left-side n-alkoxy group (Figure 1). This generated a phase diagram featuring Cr–I/Sm ,Sm-N/I , and N-I transition curves that outline the phase behavior by connecting corresponding points.

Table 2. Transition Temperature of Homologous Series D in ^{0}C.

Sr No.	No of carbon in n-alkyl chain (CnH2n+1)	Sm	N	Isotropic
1	1	-	-	220.5
2	2	-	-	210.3
3	3	-	-	213.7
4	4	-	-	194.5
5	5	-	-	197
6	6	118.6	128.8	166.8
7	7	88.9	139.7	168.6
8	8	90.7	104.6	156.4
9	10	116.2	120.7	129.2
10	12	105.4	114.3	135.4
11	14	103.2	-	118.7
12	16	103	-	122.2
	( ) monotropic, Sm = Smectic, N = Nematic			

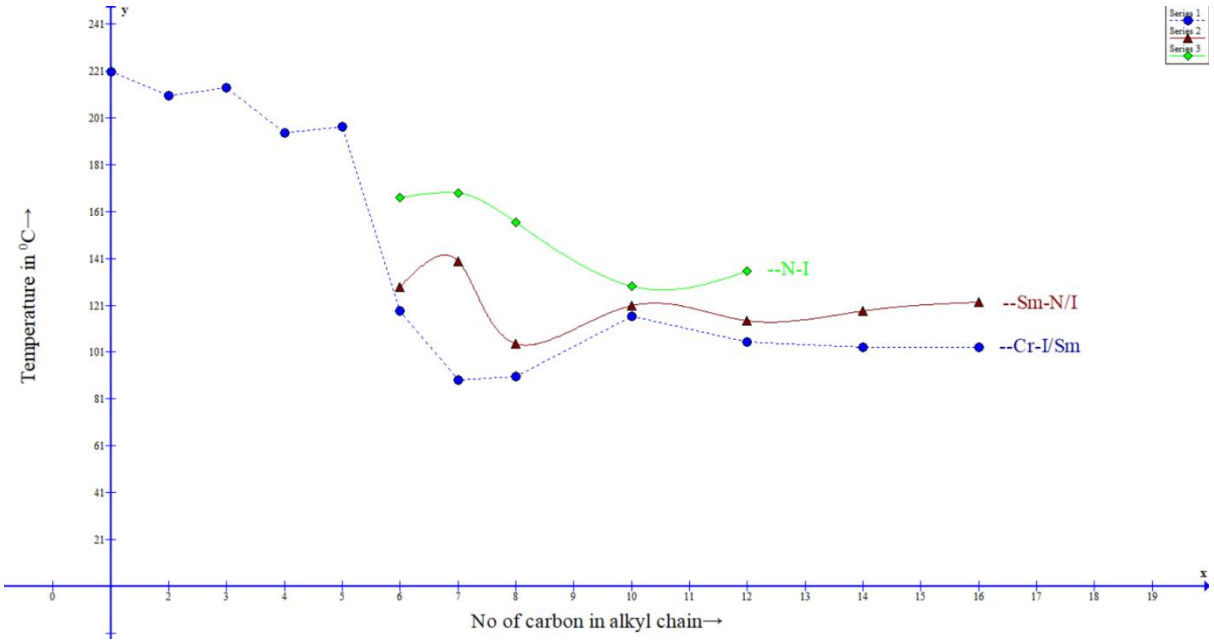

Figure 1. Phase Behaviour of Homologous Series D.

Series D contain 12 homologues. C_1 to C_5 homologues show non mesomorphic in nature while C_6 to last homologues C_{16} show mesomorphic in nature. C_6 to C_{12} homologues show poly mesomorphic in nature while C_{14} and C_{16} homologues show only smectic mesophase.

The Cr–I/Sm transition curve begins from the C_1 homologue and continues up to C_{16}. It exhibits a partialy zigzag pattern with alternating rises and falls in transition temperatures, although the overall trend shows a gradual decrease across the series.

The Sm–N/I phase transition curve, from C_6 to C_{16} homologues, shows a smooth wave-like change in transition temperatures. The temperatures go up and down from one member to the next, forming a pattern similar to a snake's movement.

Similarly, the N-I transition curve shows a decreases order except slightly rises C_7 and C_{12} homologues. Overall, the phase diagram demonstrates typical mesomorphic behaviour with irregular fluctuations but follows the expected trend across the homologues.

The thermal stability for the smectic and nematic phase of series D is 121.2ºCand 151.2ºC respectively. The smectic phase exhibits a mesomorphic range varying from 4.5 °C to 50.8 °C, whereas the nematic phase shows a range from 8.5 °C to 51.8 °C across the homologous series. Total mesophase length of smectic and nematic phase is 13.0 ºCto 79.7ºC. Analytical, spectral, and thermal data supported the molecular structures of homologues. Variations in mesogenic properties and behaviour from homologue to homologue in the same series are observed with changing number of carbon atoms in n-alkyl chain "R" of –OR group, keeping rest of the molecular part unaltered throughout the series.

The intermolecular anisotropic forces of attractions are suitable and favourably adhere as a consequence of molecular rigidity and flexibility, by molecular polarity and polarizability, so that C_6 to C_{12} all homologues of the new series exhibit liquid crystalline phases.

The homologue derivatives from hexyloxy to dodecyloxy exhibit smectic plus nematic mesophase due to the presence of lamellar packing of molecules in their crystal lattices, which causes interlinked sliding layers of molecules and statistically parallel orientational order of molecules. Homologue derivatives from C_{14} and C_{16} exhibit only Smectic mesophase due to the presence of lamellar packing of molecules in their crystal lattices.

Induced molecular polarizability by the -CF_3 group and Cyano group with a favourable length to breadth ratio, as well as end to end intermolecular attractions, favourably strengthens the intermolecular adhesion, which resulted in the formation of mesophases and a long range of mesomorphism as a consequence of favorable magnitudes of molecular rigidity and flexibility. The mesomorphic behaviour of the new series-D is compared with that of other structurally similar known series -X [29] as shown in below figure 2.

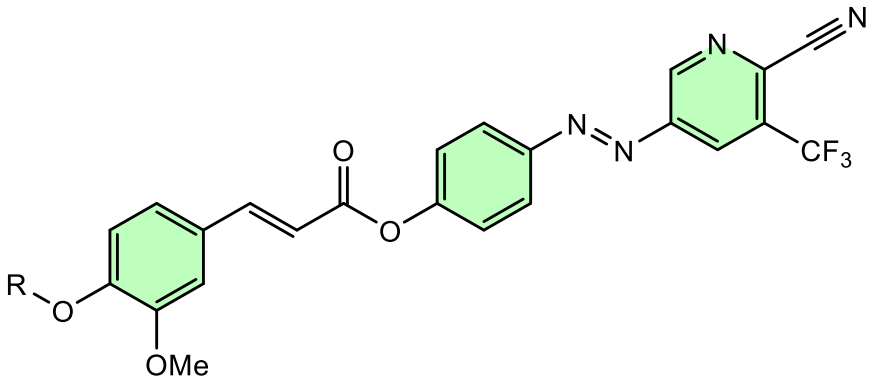

Series -D

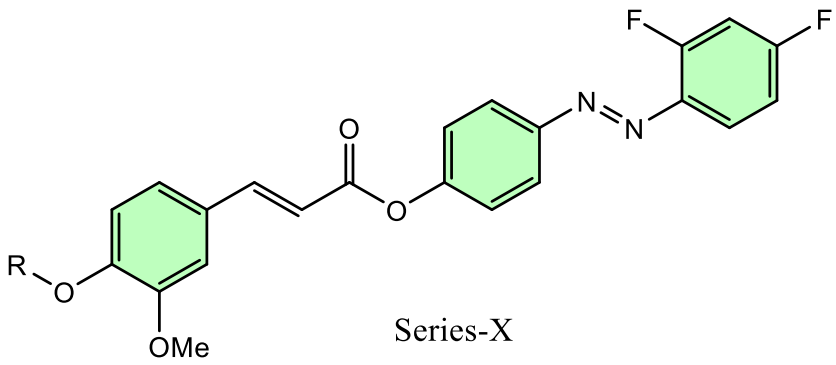

Series-X

Figure 2. Structure of Comparative Series.

The mesomorphic behaviour of Series D, 4-(4'-n-alkoxy-3'-methoxy cinnamyloxy) phenyl azo-5''-(2''-cyano-3''-trifluoromethyl) pyridine, was compared with the structurally related series (X) 4-(4'-n-alkoxy-3'-methoxy-cinnamoyloxy) phenyl azo -2''-4''-difluorobenzene . Both homologous series possess a rigid aromatic core connected through azo (–N=N–) and ester linkages, which are well known to promote anisotropic molecular shape and mesophase formation of liquid crystals. Azo-based mesogens commonly exhibit smectic and nematic phases depending on the polarity of the terminal substituents and the length of the alkoxy chain.

In Series D, the presence of strongly electron-withdrawing substituents such as cyano (–CN) and trifluoromethyl (–CF_3) groups attached to the pyridine ring significantly increases molecular polarity and dipole moment. These polar groups enhance intermolecular interactions, such as dipole–dipole forces, which improve molecular ordering and lead to relatively higher thermal stability of the mesophase. Moreover, fluorinated groups are known to increase mesomorphic stability and broaden the mesophase temperature range due to their strong inductive effect and high electronegativity.

In comparison, the difluorobenzene-based homologous series, 4-(4′-n-alkoxy-3′-methoxy cinnamoyloxy) phenylazo-2″,4″-difluorobenzene, demonstrated relatively lower mesomorphic stability. The presence of laterally substituted fluorine atoms, while enhancing dielectric anisotropy, interferes with efficient molecular packing due to both steric hindrance and electronic influences. This disruption weakens intermolecular interactions and leads to a decrease in transition temperatures. Moreover, the difluoro benzene core is less polar than the pyridine ring, which further diminishes intermolecular cohesion. As a result, this series mainly exhibits Smectic phases with comparatively narrower mesophase ranges. Another significant structural feature of Series D is the heterocyclic pyridine ring, which contains a nitrogen atom that increases molecular polarity and anisotropy. This structural characteristic favours liquid-crystalline ordering and often enhances mesophase stability compared with purely phenyl-based systems.

Overall, the comparative study clearly indicates that terminal polar groups and heterocyclic cores play a dominant role in governing mesomorphic behaviour. The combined effect of strong electron-withdrawing substituents and a pyridine nucleus leads to improved thermal stability, wider mesophase ranges, and the induction of smectic phases. In contrast, lateral fluorine substitution in a benzene-based system favours nematic behaviour with comparatively lower stability. These findings highlight the importance of molecular design in tailoring the liquid crystalline properties of azo ester derivatives for advanced applications. According to comparision of series conclusion is discuss below.

Table 3. Relative Thermal Stability In ^{0}C.

Series	D	X
Smectic-Nematic or Smectic-Isotropic	121.2°C (C_6-C_{16})	114.8°C (C_{10}–C_{16})
commencement of Smectic phase	C_6	C_{10}
Nematic-Isotropic	151.2°C (C_6 -C_{12})	-
Commencement of Nematic phase	C_6	C_4
Total mesophase length (Sm+N) in ^{0}C	13.0°C(C_{10}) to 79.7°C(C_7)	14.5°C (C_{16}) to 29.4°C(C_{10})

According to Table 3,

- The nematic and smectic thermal stability of series D is higher than compare to series X .

- In series D, the mesophase commence from the C_6 homologue, while in series X,in C_4 homologue.

- In series D, the mesophase thermal stability (Sm+N) spans from13.0ºC to 79.7 ºC. In contrast, series X exhibits smectic phase thermal stability in the range of 14.5 °C to 29.4 °C.

- Overall, the total upper and lower mesophase temperature ranges for series D is relatively higher compared to those of series X. POM optical micrographs of C_6, C_7, and C_{10} is shows in **Figure 3.**

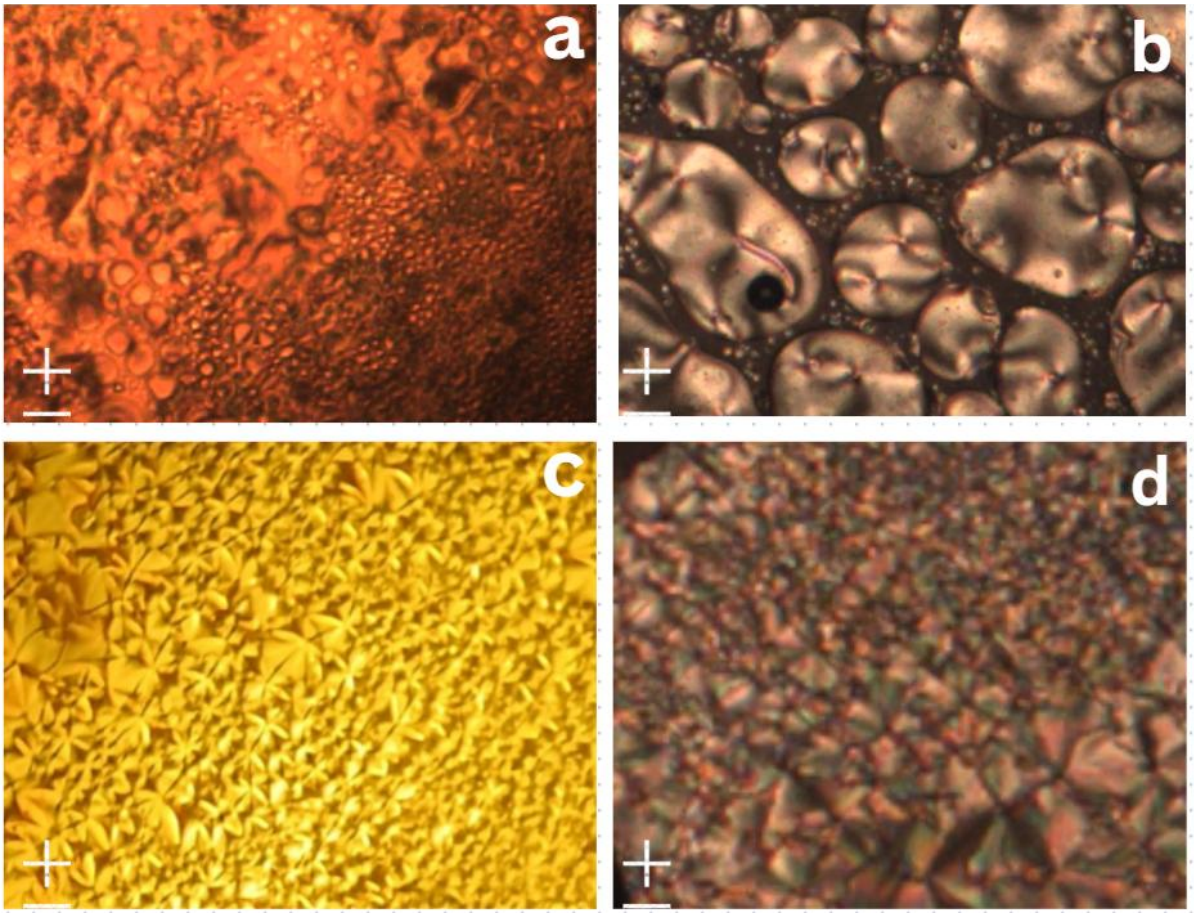

Figure a. C_6 Nematic phase on heating stage at 165.0ºC

Figure b. C_7 Nematic phase on cooling stage at 166.5 ºC

Figure c. C_6 Smectic phase on heating stage at 126 ºC

Figure d. C_{10} Smectic phase on heating stage at 119 ºC

Under polarized optical microscopy (POM), the mesophases of the investigated homologues can be effectively identified based on their distinct optical textures. Compounds D-6 and D-7 exhibit droplet-like or schlieren textures, which are characteristic of the nematic phase. Such textures arise due to the presence of long-range orientational order without any positional layering of molecules.

In contrast, compounds D-6 and D-10 show textures typical of smectic phases, including focal conic, fan-shaped, or layered structures. These features indicate a higher degree of molecular organization, where molecules are arranged in well-defined layers while maintaining orientational order.

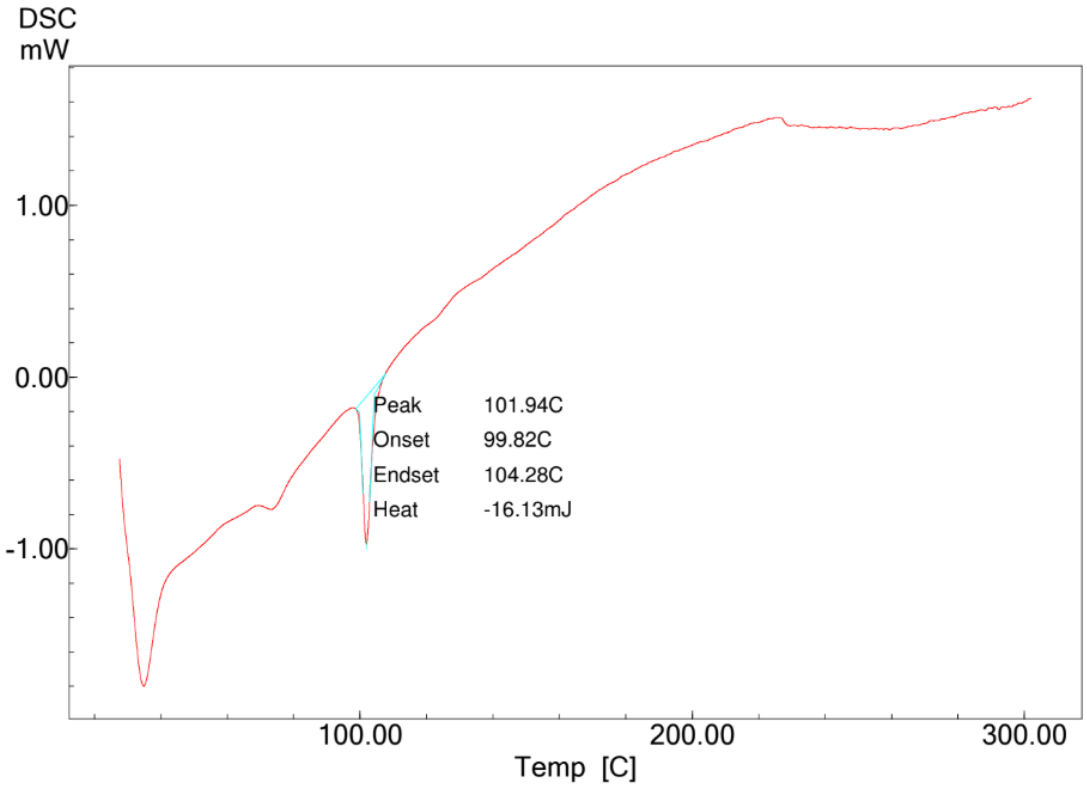

Figure 4. DSC Analysis of C_{16}.

Differential scanning calorimetry (DSC) verified the existence of nematic phases in Series D, highlighting its effectiveness in analyzing thermal transitions and associated changes in physical properties. Using a heating rate of 10 ^{0}C/min, DSC measurements provided accurate values for transition enthalpies and phase ranges of the hexadecyloxy C_{16} derivatives, as summarized in Table 4. This technique also offered insights into molecular disorder. The corresponding DSC thermograms are shown in Figure 4. Entropy changes (DS) were calculated using the formula DS ¼ DH/T, yielding values of 0.0430 mj/K for D16. The enthalpy changes (DH) for these compounds were 16.13 mj, , with phase lengths of 19.2 ^{o}Crespectively.

Conclusions

Group efficiency order derived on the basis of (I) thermal stabilities and the (II) early commencement of mesophases. Viz. smectic and nematic for lateral substitution are as under.

I. Thermal stability

Smectic: Series D > Series X

Nematic: Series D > Series-X

II. Commencement of mesophase

Smectic: Series D> Series X

Nematic: Series X > Series D

III. The total mesophase length (Sm - N)

Upper and lower:

Series D > Series X

The findings of this study provide valuable insights for the design and development of liquid crystalline materials tailored for high-temperature applications. Further explor ation of structural modifications and their impact on mesomorphic behavior could lead to the creation of more efficient and tunable liquid crystalline materials.

Acknowledgments

The authors are thankful to the Department of Chemistry, Saurashtra University, Rajkot, Gujarat (India) for providing facilities.

References

[1] P. Kumar Choudhury and A.-B. M.A. Ibrahim, "Introductory Chapter: Liquid Crystals and Applications," in *Liquid Crystals*, P. Kumar Choudhury and A.-B. M.A. Ibrahim, Eds., IntechOpen, 2022. doi: 10.5772/intechopen.105105.

[2] H. K. Bisoyi and Q. Li, "Liquid Crystals: Versatile Self-Organized Smart Soft Materials," *Chem. Rev.*, vol. 122, no. 5, pp. 4887–4926, Mar. 2022, doi: 10.1021/acs.chemrev.1c00761.

[3] N. Khatun, A. C. Nkele, and K. Bagchi, "Liquid crystals as solid-state templates," *Phys. Chem. Chem. Phys.*, vol. 27, no. 13, pp. 6408–6424, 2025, doi: 10.1039/D4CP04526B.

[4] K. P. Zuhail, M. Humar, and S. Dhara, "Effect of phase transitions on liquid crystal colloids: a short review," *Liquid Crystals Reviews*, vol. 8, no. 1, pp. 44–57, Jan. 2020, doi: 10.1080/21680396.2021.1904298.

[5] C.-H. Chen and I. Dierking, "Nanoparticles in thermotropic and lyotropic liquid crystals," *Front. Soft Matter*, vol. 4, p. 1518796, Jan. 2025, doi: 10.3389/frsfm.2024.1518796.

[6] Kato, T., Uchida, J., Ichikawa, T., & Sakamoto, T. (2022). Functional liquid crystals towards the next generation of materials. *Angewandte Chemie International Edition, 61*(22), e202200123. https://doi.org/10.1002/anie.202200123

[7] Lee, K. M., Marsh, Z. M., Crenshaw, E. P., Tohgha, U. N., Ambulo, C. P., Wolf, S. M., … Godman, N. P. (2023). Recent advances in electro-optic response of polymer-stabilized cholesteric liquid crystals. *Materials, 16*(6), 2248. https://doi.org/10.3390/ma16062248

[8] Wu, H., Jiang, Y., Hu, W., Feng, S., & Li, J. (2023). Effect of mesogenic phase and structure of liquid crystals on tribological properties as lubricant additives. *Coatings, 13*(1), 168. https://doi.org/10.3390/coatings13010168

[9] Tschierske, C. (2023). Development of structural complexity by liquid-crystal self-assembly. *Chemical Society Reviews, 52*(3), 1234–1302. https://doi.org/10.1039/D2CS00745A

[10] Patel, R. B., Doshi, A. V., & Vyas, N. N. (2022). Synthesis and mesomorphic properties of azo ester-based liquid crystals: Effect of terminal substituents. *Liquid Crystals, 49*(8), 987–998. https://doi.org/10.1080/02678292.2022.2045678

[11] Lee, K. M., Marsh, Z. M., Crenshaw, E. P., Tohgha, U. N., Ambulo, C. P., Wolf, S. M., … Godman, N. P. (2023). Recent advances in electro-optic response of polymer-stabilized cholesteric liquid crystals. *Materials, 16*(6), 2248. https://doi.org/10.3390/ma16062248

[12] Kim, Y., & Lee, M. (2022). Supramolecular liquid crystals: from thermotropic to lyotropic systems. *Materials Horizons, 9*(6), 1500–1520. https://doi.org/10.1039/D2MH00123K

[13] Ahmed, H. A., Naoum, M. M., & Saad, G. R. (2023). Mesophase behavior of new Schiff base/ester liquid crystals: Impact of molecular structure. *Crystals, 13*(2), 245. https://doi.org/10.3390/cryst13020245

[14] Aziz, T., Nasim, H. A., Ahmad, K., Shah, H. U. R., Parveen, S., Ahmad, M. M., et al. (2022) Rational synthesis and biological evaluation of azo derivatives of phenylcarbonyl diazinyl heterocycles. *Heliyon, 9*(1), e12492. https://doi.org/10.1016/j.heliyon.2022.e12492

[15] Xiong, D., Xiong, X., Chen, Z., Yu, W., & Feng, C. (2022). Mesophase behaviour of 1,2,3-triazole-based nematic liquid crystals influenced by varying alkyl chains and halogen atom substitution. *Liquid Crystals, 49*(10), 1–12. https://doi.org/10.1080/02678292.2022.2066731

[16] Rabari, M., Hegde, V., Hegde, G., & Prajapati, A. K. (2025). Unsymmetrical mesogenic cyanobiphenyl dimers: Mesomorphic, photo-switching and structural studies. *Journal of Materials Chemistry C, 13*, 10700–10713. https://doi.org/10.1039/D5TC00421G

[17] Kumar, S., et al. (2025). Coumarin-based fluorescent liquid crystal dimers: Mesogenic and photophysical behavior. *Journal of Molecular Liquids, 417*, 126691 https://doi.org/10.1016/j.molliq.2024.126691

[18] Kelly, S. M. (2024). Liquid crystalline materials containing pyrimidine and pyridine rings. *Liquid Crystals, 51*(10), 1617–1650. https://doi.org/10.1080/02678292.2024.2361294

[19] Xiong, D., Xiong, X., Chen, Z., Yu, W., & Feng, C. (2022).
Mesophase behaviour of triazole-based liquid crystals influenced by structural variation. *Liquid Crystals, 49*(10), 1261–1274. https://doi.org/10.1080/02678292.2022.2066731

[20] Mandle, R. J., et al. (2024). Sulfur-linked liquid crystal dimers and the twist-bend nematic phase. *Physical Chemistry Chemical Physics*.
https://doi.org/10.1039/D4CP04189E

[21] El-Seify, F. A., Azab, H. A., Degedy, F. S., Abdel-Mageed, K. A., & El-Dossoki, F. I. (2022). Physico-analytical studies on heterocyclic azo dyes and their complexes. *BMC Chemistry, 16*, 40.https://doi.org/10.1186/s13065-022-00833-x

[22] Kamal, S. J., Salleh, N. M., Mahmud, H. N. M. E., & Zahid, N. I. (2021). Liquid crystal and photophysical properties of laterally fluorinated azo-ester materials. *Liquid Crystals, 49*(5), 633–646. https://doi.org/10.1080/02678292.2021.1995060

[23] Mehmood, H., Iqbal, M. A., Ashiq, M. N., & Hua, R. (2021). Base-promoted one-pot synthesis of pyridine derivatives via aromatic alkyne annulation using benzamides as nitrogen source. *Molecules, 26*(21), 6599. https://doi.org/10.3390/molecules26216599

[24] Zala, P. P., & Bhoya, U. C. (2024).
Synthesis and characterization of new thermotropic liquid crystalline compounds with azo-vinyl ester linkages. *World Scientific News*.

[25] Ahmed, H. A., Hagar, M., & Alnoman, R. B. (2022).
The influence of molecular flexibility on the mesogenic behavior of a new homologous series based on azo-azomethine: Synthesis, characterization, photoisomerization and DFT study. *Journal of Molecular Structure, 1249*, 131586. https://doi.org/10.1016/j.molstruc.2021.131586

[26] Youssef, M. M., Abd El-Latif, M. M., & Mohamed, G. G. (2022).
Synthesis and mesomorphic properties of new azo ester liquid crystals derived from substituted benzaldehydes. *Liquid Crystals, 49*(10), 1302–1313.
https://doi.org/10.1080/02678292.2022.2041234

[27] Khan, M. F., et al. (2025).
Synthesis, characterization, and biological evaluation of novel azo-based imidazo[1,2-a]pyridine derivatives. *ACS Omega*. https://doi.org/10.1021/acsomega.5c07351

[28] Dave, J. S., & Vora, R. A. (1970).
In *Liquid Crystals and Ordered Fluids* (Eds. J. F. Johnson & R. S. Porter), Plenum Press, New York, pp. 477–496. https://doi.org/10.1007/978-1-4684-8214-0

[29] B. Bodar and U. Bhoya, "Influence of difluoro substitution on the mesomorphic and thermal behavior of azo-cinnamate ester liquid crystals: experimental and DFT analysis," *Molecular Crystals and Liquid Crystals*, pp. 1–21, Mar. 2026, doi: 10.1080/15421406.2026.2649213